

PREPARED FOR SUBMISSION TO JHEP

# Exact WKB and the quantum Seiberg-Witten curve for 4d $N = 2$ pure $SU(3)$ Yang-Mills, Part I: Abelianization

---

Fei Yan<sup>1</sup>

<sup>1</sup>*NHETC and Department of Physics and Astronomy, Rutgers University*

*E-mail:* [fyan.hepth@gmail.com](mailto:fyan.hepth@gmail.com)

**ABSTRACT:** We investigate the exact WKB method for the quantum Seiberg-Witten curve of 4d  $N = 2$  pure  $SU(3)$  Yang-Mills, in the language of abelianization. The relevant differential equation is a third-order equation on  $\mathbb{CP}^1$  with two irregular singularities. Exact WKB analysis leads us to consider new Darboux coordinates on a moduli space of flat  $SL(3, \mathbb{C})$ -connections. In particular, in the weak coupling region we encounter coordinates of higher length-twist type generalizing Fenchel-Nielsen coordinates. The Darboux coordinates are conjectured to admit asymptotic expansions given by the formal quantum periods series; we perform numerical analysis supporting this conjecture.

---

## Contents

<b>1</b>	<b>Introduction</b>	<b>2</b>
1.1	Supersymmetric gauge theories and quantum mechanical systems	2
1.1.1	The gauge/Bethe correspondence	2
1.1.2	The topological string/spectral theory correspondence	3
1.1.3	Opers and the conformal limit	4
1.2	Different methods to compute resummed quantum periods	4
1.2.1	Computing quantum periods via abelianization	6
1.2.2	Computing quantum periods via TBA-like integral equations	7
1.2.3	Computing quantum periods via instanton calculus	7
1.3	The $SU(3)$ equation	8
<b>2</b>	<b>Exact WKB and abelianization for <math>SL(3)</math>-opers</b>	<b>9</b>
2.1	The WKB solutions	10
2.2	Abelianization	12
2.3	The spectral coordinates	13
<b>3</b>	<b>The <math>SU(3)</math> equation in the strong-coupling region</b>	<b>15</b>
3.1	The BPS spectrum	15
3.2	Stokes graphs	16
3.3	Solving the abelianization problem	17
3.4	The spectral coordinates	19
3.5	The asymptotic behavior	19
<b>4</b>	<b>The <math>SU(3)</math> equation in the weak-coupling region</b>	<b>21</b>
4.1	A Stokes graph	21
4.2	Solving the abelianization problem	22
4.3	The spectral coordinates	23
4.4	The asymptotic behavior	24

---

# 1 Introduction

Recently many interesting relations have been discovered between quantum mechanical systems and supersymmetric gauge theories (e.g. [1–13]). In particular, these relations provide tools to study the quantization of Seiberg-Witten curves [14, 15] of 4d  $N = 2$  theories, in various different contexts. Our goal in this paper and its follow up [16], is to study the quantum Seiberg-Witten curve of 4d  $N = 2$  pure  $SU(3)$  super Yang-Mills (SYM) theory via different approaches.

## 1.1 Supersymmetric gauge theories and quantum mechanical systems

We begin with a review of correspondences between supersymmetric gauge theories and quantum mechanical systems from three different perspectives.

### 1.1.1 The gauge/Bethe correspondence

The first perspective arises in the context of gauge/Bethe correspondence [1, 17, 18], where 4d  $N = 2$  gauge theories in the  $\Omega$ -background provide the quantization of certain classical integrable systems. Concretely, one takes the Nekrasov-Shatashvili (NS) limit with  $\epsilon_1 = \hbar$  and  $\epsilon_2 \rightarrow 0$ , the low energy effective theory is a 2d  $N = (2, 2)$  theory with an effective twisted superpotential:

$$\widetilde{W}_{\text{eff}}(\mathbf{a}, \hbar) = \lim_{\epsilon_2 \rightarrow 0} \epsilon_2 \log Z(\mathbf{a}, \epsilon_1 = \hbar, \epsilon_2), \quad (1.1)$$

where  $Z(\mathbf{a}, \epsilon_1, \epsilon_2)$  is the 4d Nekrasov partition function in  $\Omega$ -background [19, 20]. Here  $\mathbf{a}$  correspond to the vacuum expectation values of complex scalars in the  $N = 2$  vector multiplets. The effective 2d theory has a discrete set of vacua corresponding to solutions to

$$\exp \left( \frac{\partial \widetilde{W}_{\text{eff}}(\mathbf{a}, \hbar)}{\partial a_i} \right) = 1, \quad i = 1, \dots, r \quad (1.2)$$

where  $r$  is the rank of the 4d theory. In the context of quantum integrable systems,  $\widetilde{W}_{\text{eff}}(\mathbf{a}, \hbar)$  is identified with the Yang-Yang functional, and equation (1.2) is the Bethe equation determining the set of eigenvalues of mutually commuting Hamiltonians.

There is a special class of 4d  $N = 2$  theories called class  $S$  theories  $\mathcal{T}(\mathfrak{g}, C)$ , which are obtained by compactifying 6d  $(2, 0)$  theory of type  $\mathfrak{g}$  on a Riemann surface  $C$  with a partial topological twist [21, 22]. Subjecting a class  $S$  theory to  $\Omega$ -deformation in the NS limit [1, 23] gives quantization of the corresponding Hitchin integrable system where the phase space is the moduli space  $\mathcal{M}_H(\mathfrak{g}, C)$  of solutions to Hitchin's equations on the Riemann surface  $C$  [24].

In this context, the Seiberg-Witten curve of the class  $S$  theory is quantized to an *oper* [25], which is certain meromorphic differential operator on  $C$ . For example, take  $\mathfrak{g} = A_{N-1}$ , an oper in a class  $S$  theory of type  $A_{N-1}$  could be written as the following  $N$ -th order meromorphic operator on  $C$ :

$$\mathcal{O}_N(z) := \partial_z^N + t_2(z, \hbar) \partial_z^{N-2} + \cdots + t_N(z, \hbar). \quad (1.3)$$

Moreover, the variety of opers is a  $\hbar$ -dependent Lagrangian submanifold in  $\mathcal{M}_H(\mathfrak{g}, C, \hbar)$ ; it provides the quantization of Coulomb branch of the class  $S$  theory.

In [3] it was proposed that, for a class  $S$  theory  $\mathcal{T}(A_{N-1}, C)$ , there exists a specific Darboux coordinate system, where the generating function for the variety of opers is identified with the effective twisted superpotential, up to certain boundary contribution at infinity. This is often called the NRS conjecture. As studied in [3], for  $N = 2$  such coordinates are complexified Fenchel-Nielsen coordinates [26]. Some examples of  $N > 2$  have been explored in [8, 27], where the relevant Darboux coordinates are higher-rank analogues of Fenchel-Nielsen coordinates. In particular, [8] gave a gauge-theoretic derivation of NRS conjecture and its generalization to the  $N = 3$  case, by studying certain 1/2-BPS codimension two surface defects in the 4d  $N = 2$  theory. Concretely, the non-perturbative Dyson-Schwinger equation [7] satisfied by the surface defect partition function gives a quantized version of opers; it reduces to the oper equation in the NS limit.

### 1.1.2 The topological string/spectral theory correspondence

Another interesting development is the topological string/spectral theory (TS/ST) correspondence [5, 6, 28], which associates a non-perturbative quantum mechanical operator to a toric Calabi-Yau manifold. The relevant spectral problem is associated with the quantization scheme for mirror curves to the toric Calabi-Yau manifold. In particular, explicit expressions for the spectral determinant could be written down using a 11d version of the topological string free energy [5], which allows the derivation of exact quantization condition for the operator spectrum.

To make contact with 4d  $N = 2$  theories, one uses geometric engineering methods [29], taking certain limit of topological string theory on appropriate Calabi-Yau geometry [11, 30]. Quantization of the Seiberg-Witten curve arises as the *canonical quantization* of an algebraic curve. As an example, [30] studied a deformed Hamiltonian in quantum mechanics, which arises in the context of quantization of Seiberg-Witten curves (as hyperelliptic curves [14, 31–33]) for 4d  $N = 2$  pure  $SU(N)$  SYM. A conjectural exact quantization condition was written down in closed form, using the 4d limit of TS/ST correspondence.

### 1.1.3 Opers and the conformal limit

There is yet another way, introduced in [4], to describe the quantization of the Coulomb branch of class  $S$  theories in terms of the variety of opers.

As described in [21], compactifying a class  $S$  theory  $\mathcal{T}(\mathfrak{g}, C)$  on a circle with radius  $R$ , the low energy effective theory is a 3d  $N = 4$  sigma model with target space being Hitchin moduli space  $\mathcal{M}_H(\mathfrak{g}, C)$ . Note that the radius  $R$  of the compactification circle is a parameter in the corresponding Hitchin's equations.  $\mathcal{M}_H(\mathfrak{g}, C)$  has a  $\mathbb{CP}^1$ -worth of complex structures parametrized by  $\zeta$ , where at  $\zeta = 0$  the moduli space is a complex integrable system. It is described as a torus fibration over the Coulomb branch of the 4d theory, where the torus fibre parameterize choice of Wilson lines and 't Hooft lines around the circle. With respect to the complex structure at  $\zeta = 0$ , there is a canonical Lagrangian submanifold  $\mathcal{L}$ , corresponding to the locus in  $\mathcal{M}_H(\mathfrak{g}, C)$  where the Wilson and 't Hooft lines are turned off;  $\mathcal{L}$  is canonically isomorphic to the 4d Coulomb branch.

The quantization of 4d Coulomb branch in this setup happens in a special scaling limit, the so-called *conformal limit* [4], where one sends both  $\zeta$  and  $R$  to 0 while keeping  $\hbar = \zeta/R$  fixed. Viewing  $\mathcal{M}_H(\mathfrak{g}, C)$  as a complex symplectic manifold in complex structure  $\zeta$ , the conformal limit is a well-defined scaling limit, and one denotes the resulting complex symplectic manifold as  $\mathcal{M}_H(\mathfrak{g}, C; \hbar)$ . Let  $\mathcal{L}_\hbar$  be the image of  $\mathcal{L}$  under the conformal limit, the statement is that  $\mathcal{L}_\hbar$  is a Lagrangian submanifold in  $\mathcal{M}_H(\mathfrak{g}, C; \hbar)$ , moreover it was conjectured to coincide with the variety of opers. The physical motivation behind this conjecture was through twisted compactification of the 4d theory on  $\Omega_\hbar$ -deformed cigar-like geometry [23], where  $\mathcal{L}_\hbar$  is associated with the boundary condition at the tip of the cigar. This conjecture was demonstrated to be true in various examples, in [4] and subsequent work such as [9–11, 34–36]. From a mathematical point of view, this conjecture was proven in some cases in [37].

From a computational point of view, the conjecture in [4] offers new methods to study the quantum Seiberg Witten curves of class  $S$  theories. In particular, the conformal limit connects the exact WKB methods for opers with the exact WKB methods for flat connections parametrized by  $R$  and  $\zeta$ ; these methods were developed in [21, 38]. Concretely the Stokes graphs appearing in exact WKB for opers are the same as the *spectral networks* introduced in [38]. This philosophy was further explored in [10], which described the exact WKB method in the language of abelianization; we will give an overview of their methods in Section §2.

## 1.2 Different methods to compute resummed quantum periods

In Section §1.1 we reviewed three setups where quantization of Seiberg-Witten curves occurs; this motivates different methods to compute the corresponding properly re-

summed *quantum periods*. Computing quantum periods using these different methods and checking their agreements (see e.g. [11]), is an important tool in understanding the correspondences between 4d  $N = 2$  gauge theories and quantum mechanical systems. In this paper and [16], we aim to generalize such analysis to higher rank theories, using 4d  $N = 2$  pure  $SU(3)$  SYM as a concrete example.

Let us consider the quantum Seiberg-Witten curve for a class  $S$  theory  $\mathcal{T}(A_{N-1}, C)$ , namely we look at the differential equation corresponding to an  $SL(N)$ -oper in (1.3):

$$[\partial_z^N + t_2(z, \hbar) \partial_z^{N-2} + \cdots + t_N(z, \hbar)] \psi(z) = 0. \quad (1.4)$$

The standard WKB method makes the following ansatz for the wavefunction  $\psi(z)$ :

$$\psi(z) = \exp\left(\frac{1}{\hbar} \int_{z_0}^z \lambda(z) dz\right) \quad (1.5)$$

Substituting (1.5) into (1.4) yields an order- $N$  analogue of the Riccati equation. The first step in constructing a solution is building a formal series solution to the Riccati equation in powers of  $\hbar$ . At order- $\hbar^0$ , the relevant equation describes the classical Seiberg-Witten curve for  $\mathcal{T}(A_{N-1}, C)$ , as a  $N$ -fold branched covering  $\tilde{C} \rightarrow C$ . There are  $N$  choices of order- $\hbar^0$  solutions; they correspond to the  $N$  sheets of the Seiberg-Witten curve  $\tilde{C}$ . We choose a sheet  $i$  and consider the formal series solution

$$\lambda_i^{\text{formal}}(\hbar) = \sum_{n=0}^{\infty} \lambda_i^{(n)} \hbar^n, \quad (1.6)$$

where  $\lambda_i^{(0)}$  is an order- $\hbar^0$  solution. The higher order  $\lambda_i^{(n)}$  are then uniquely fixed by recursively solving the Riccati equation in orders of  $\hbar$ .

Classical periods of the Seiberg-Witten curve are given by the integrals of  $\lambda^{(0)}$  along 1-cycles  $\gamma$  of  $\tilde{C}$ , where  $\gamma$  labels the IR electromagnetic (and flavor) charge. Correspondingly, the quantum periods or WKB periods are defined as

$$\Pi_\gamma(\hbar) := \oint_\gamma \lambda^{\text{formal}}(\hbar) dz, \quad \gamma \in H_1(\tilde{C}, \mathbb{Z}), \quad (1.7)$$

where  $\Pi_\gamma(\hbar)$  is a formal power series in  $\hbar$

$$\Pi_\gamma(\hbar) = \sum_{n=0}^{\infty} \Pi_\gamma^{(n)} \hbar^n, \quad \Pi_\gamma^{(n)} = \oint_\gamma \lambda^{(n)} dz. \quad (1.8)$$

$\Pi_\gamma^{(n)}$  in general diverges as  $n!$  [11, 39–41]; a natural way to properly resum  $\Pi_\gamma(\hbar)$  is the Borel resummation. There could be rays in the Borel plane along which the

Borel transform has singularities. As a consequence,  $\Pi_\gamma(\hbar)$  is not Borel summable for certain phases of  $\hbar$ . One could nevertheless define lateral Borel resummations by slightly deforming the integration contour below or above the ray corresponding to such a phase. These two choices of deformation produce different answers, where the difference is defined as the *Stokes discontinuity* of quantum periods. Borel resummation of quantum periods and their associated Stokes discontinuities have a very rich structure, which has been an important topic in resurgence theory.

The correspondences between gauge theories and quantum mechanical systems reviewed in Section §1.1 motivate alternative ways to compute resummed quantum periods, which we describe below.

### 1.2.1 Computing quantum periods via abelianization

Motivated by developments reviewed in §1.1.3, exact WKB methods could be reformulated geometrically in the context of *abelianization* [10, 27, 38, 42], which maps a flat  $\mathrm{SL}(N, \mathbb{C})$ -connection over the Riemann surface  $C$  to a flat  $\mathrm{GL}(1, \mathbb{C})$ -connection over the Seiberg-Witten curve  $\tilde{C} \rightarrow C$ . The Borel resummed quantum periods are closely related to the *Voros symbols*  $\mathcal{X}_\gamma(\hbar)$ <sup>1</sup>, defined as holonomy of the flat abelian connection along 1-cycles  $\gamma$  in  $\tilde{C}$ .

Using abelianization methods,  $\mathcal{X}_\gamma(\hbar)$  can be explicitly written as products of Wronskians of distinguished local solutions to the oper equation (1.4). In this way  $\mathcal{X}_\gamma(\hbar)$  could be identified as *spectral coordinates* on a moduli space of flat  $\mathrm{SL}(N, \mathbb{C})$ -connections. In the case of  $\mathrm{SL}(2)$ -opers, in generic situations  $\mathcal{X}_\gamma(\hbar)$  are Fock-Goncharov coordinates [21, 43]; less generically one could also obtain exponentiated complexified Fenchel-Nielsen coordinates [3, 26, 42]. In the case of higher-rank  $\mathrm{SL}(N)$ -opers, in special cases  $\mathcal{X}_\gamma(\hbar)$  could be identified with higher-rank Fock-Goncharov coordinates [38, 43] or higher length-twist coordinates [8, 27] generalizing Fenchel-Nielsen coordinates. In general though, abelianization for higher-rank opers spells out spectral coordinates that haven't been studied before.

The connection between  $\mathcal{X}_\gamma(\hbar)$  and quantum periods is mediated by certain asymptotic properties of  $\mathcal{X}_\gamma(\hbar)$  motivated from [4, 10, 21, 38]. In particular, as  $\hbar \rightarrow 0$  while staying within certain half of the  $\hbar$ -plane,  $\log(\mathcal{X}_\gamma(\hbar))$  admits an asymptotic expansion

$$\log(\mathcal{X}_\gamma(\hbar)) \sim \frac{1}{\hbar} \Pi_\gamma(\hbar), \quad (1.9)$$

where  $\Pi_\gamma(\hbar)$  is the formal series of quantum periods defined in (1.7). Moreover if  $\hbar \rightarrow 0$  along the central ray within the half-plane,  $\hbar \log(\mathcal{X}_\gamma(\hbar))$  produces the Borel resummed

---

<sup>1</sup>More precisely the Voros symbol depends on a phase parameter  $\theta$ . Detailed definitions are described in Section §2.

quantum periods.<sup>2</sup>

For  $SL(2)$ -opers, mathematically speaking such asymptotic behavior of Voros symbols has been proven by Koike-Schäfer; for higher  $SL(N)$ -opers though it remains to be a conjecture. Certain numerical evidence for this conjecture had been provided in [10, 36]. In this paper we provide further evidence in the concrete example of an  $SL(3)$ -oper which appears in the quantization of Seiberg-Witten curve of 4d  $N = 2$  pure  $SU(3)$  SYM.

### 1.2.2 Computing quantum periods via TBA-like integral equations

The spectral coordinates  $\mathcal{X}_\gamma(\hbar)$  obey certain TBA-like integral equations [4], which could be viewed as the conformal limit of the TBA-like integral equations in [44]. These integral equations are very useful in the study of quantum periods.

There exists an interesting correspondence between BPS states and resurgent properties of quantum periods [4, 9, 11, 35]. Singularities of Borel transform for quantum periods are controlled by BPS spectrum of the 4d theory. Moreover the Stokes discontinuities of quantum periods are closely related to the Kontsevich-Soibelman transformation [21, 44, 45]. As a consequence, the integral equations predict the locations of singularities in the Borel plane and the discontinuities in lateral Borel resummations of quantum periods.

The Borel resummed quantum periods are solutions to the integral equations; in principal one can compute them by solving the integral equations iteratively, after specifying boundary conditions on the solutions. This perspective has been explored in various examples in [5, 9–11, 36].

### 1.2.3 Computing quantum periods via instanton calculus

The NS limit [1] of instanton calculus [19] also provides a resummation of quantum periods [11, 46]. Concretely instanton calculus picks up distinguished quantum periods: the quantum  $A$ - and  $B$ -periods  $\{a_1(\hbar), \dots, a_r(\hbar), a_D^1(\hbar), \dots, a_D^r(\hbar)\}$ <sup>3</sup> satisfying the quantum special geometry relation

$$a_D^i(a_1, \dots, a_r; \hbar) = \frac{\partial F_{\text{NS}}(a_1, \dots, a_r; \hbar)}{\partial a_i}, \quad i = 1, \dots, r \quad (1.10)$$

Here  $F_{\text{NS}}(a_1, \dots, a_r; \hbar)$  is the Nekrasov-Shatashvili free energy [1], which is  $\hbar$  times the effective twisted superpotential  $\widetilde{W}_{\text{eff}}$ . This free energy is given as a power series in

---

<sup>2</sup>If  $\Pi_\gamma(\hbar)$  happens to be not Borel-summable, then  $\hbar \log(\mathcal{X}_\gamma(\hbar))$  is conjectured to produce the median Borel summation of  $\Pi_\gamma(\hbar)$  [10].

<sup>3</sup>Here  $r$  denotes the rank of the theory.



the instanton counting parameter with a non-vanishing convergence radius in certain parameter range around the semiclassical region.

Given the NS free energy, the quantum  $A$ -periods  $a_i(\hbar)$  could be obtained by inverting the quantum Martone relation [47–49]. The quantum  $B$ -periods  $a_D^i(\hbar)$  are then computed via (1.10). For appropriate parameter range, both  $a_i(\hbar)$  and  $a_D^i(\hbar)$  are convergent series expansion in the counting parameter with non-zero convergence radius, in particular they are exact in  $\hbar$ . Instanton calculus thus provides a natural resummation for the quantum  $A$ - and  $B$ -periods.<sup>4</sup>

The NRS conjecture and its higher rank generalization [3, 8, 27] suggests that the instanton resummed quantum  $A$ - and  $B$ -periods correspond to certain specific spectral coordinates: the Fenchel-Nielsen coordinates or higher length-twist coordinates. Symbolically<sup>5</sup> one expects the following relation in the higher rank case:

$$\log(\mathcal{X}_\gamma^{\text{length}}(\hbar)) = \frac{1}{\hbar}a(\hbar), \quad \log(\mathcal{X}_\gamma^{\text{twist}}(\hbar)) = \frac{1}{\hbar}a_D(\hbar). \quad (1.11)$$

### 1.3 The $SU(3)$ equation

In this paper and its followup [16], we investigate the quantum Seiberg-Witten curve for the  $N = 2$  pure  $SU(3)$  super Yang-Mills. Some related work in this theory has appeared before in [30, 50]. Here we start with the canonical Seiberg-Witten curve appearing in the class- $S$  construction of  $N = 2$  pure  $SU(3)$  SYM, via compactifying a 6d (2,0) theory of type  $A_2$  on  $\mathbb{CP}^1$  with two irregular singularities at  $z = 0$  and  $z = \infty$ . The quantization of this Seiberg-Witten curve leads us to study the following third-order differential equation:

$$\left[ \partial_z^3 + \hbar^{-2} \frac{u_1}{z^2} \partial_z + \left( \hbar^{-3} \left( \frac{\Lambda}{z^4} + \frac{u_2}{z^3} + \frac{\Lambda}{z^2} \right) - \hbar^{-2} \frac{u_1}{z^3} \right) \right] \psi(z) = 0, \quad (1.12)$$

where  $u_1$  and  $u_2$  are Coulomb branch parameters. We denote this equation as the  $SU(3)$  equation.

As discussed in §1.2, there are different methods to compute properly resummed quantum periods in this theory. In this paper we focus on the method described in §1.2.1, namely we compute Borel resummed quantum periods via abelianization. In the followup [16], we intend to investigate the TBA method described in §1.2.2 and the instanton calculus method described in §1.2.3.

---

<sup>4</sup>Relation between instanton resummation and Borel resummation has been clarified in [11], in the context of  $N = 2$  pure  $SU(2)$  SYM.

<sup>5</sup>There could be certain ambiguities in FN or higher length-twist coordinates, corresponding to certain monodromy action mixing  $a$  with  $a_D$ . We thank Andrew Neitzke for pointing this out.

Concretely we study loci in both the strong-coupling region and the weak-coupling region. In the strong-coupling chamber with 12 BPS states, the Voros symbol  $\mathcal{X}_\gamma(\hbar)$  could be expressed in terms of Wronskians of distinguished local solutions to (1.12), which decay exponentially as one goes into the irregular singularity at  $z = 0$  or  $z = \infty$ .  $\mathcal{X}_\gamma(\hbar)$  are certain coordinates for flat  $\mathrm{SL}(3, \mathbb{C})$ -connections over  $\mathbb{CP}^1$  with two irregular singularities; such coordinates haven't been considered before as far as we know. We also numerically evaluate  $\log(\mathcal{X}_\gamma(\hbar))$  and compare with the expected asymptotic quantum periods expansion to certain order in  $\hbar$ . We find relatively good numerical agreement; we view this as evidence that higher-order exact WKB analysis does work.

We also investigate certain loci in the weak-coupling region, where  $\mathcal{X}_\gamma(\hbar)$  is expressed using exponentially decaying local solutions as one goes into an irregular singularity, as well as eigenvectors of the monodromy around the irregular singularity. The  $\mathcal{X}_\gamma(\hbar)$  constructed in the weak-coupling region is an instance of the higher length-twist coordinates. Different from examples in [8, 27], here  $\mathcal{X}_\gamma(\hbar)$  are coordinates on a moduli space of flat  $\mathrm{SL}(3, \mathbb{C})$ -connections over a surface containing irregular singularities. We perform numerical check against the expected asymptotic quantum periods expansion. Additionally we comment on the exact quantization condition (EQC) for a bound state problem associated with the differential equation (1.12).

Finally we remark that, it would be very interesting to have a gauge-theoretical derivation of higher length-twist coordinates in this example and understand the generalized NRS conjecture, by studying 1/2-BPS codimension two surface defects in the  $N = 2$  pure  $SU(3)$  theory, following the work of [8].

## 2 Exact WKB and abelianization for $\mathrm{SL}(3)$ -opers

In [10, 38] a geometric reformulation of exact WKB has been proposed, for Schrödinger operators and higher order opers. A key ingredient in this reformulation is a process of *abelianization*, which maps a flat  $\mathrm{SL}(N, \mathbb{C})$ -connection over a Riemann surface  $C$  to a flat  $\mathrm{GL}(1, \mathbb{C})$ -connection over a  $N$ -fold covering  $\tilde{C} \rightarrow C$ . In this section we review exact WKB analysis in the language of abelianization. Our description here follows closely [10].

Concretely we focus on the case of  $\mathrm{SL}(3)$ -opers, namely an third-order differential equation involving two meromorphic potentials  $P_2(z)$  and  $P_3(z)$ <sup>6</sup>:

$$\left[ \partial_z^3 + \hbar^{-2} P_2(z) \partial_z + \left( \hbar^{-3} P_3(z) + \frac{1}{2} \hbar^{-2} P_2'(z) \right) \right] \psi(z) = 0. \quad (2.1)$$

---

<sup>6</sup>For the examples we study here,  $P_2$  and  $P_3$  are independent of  $\hbar$ .

Although this equation is written explicitly in a single coordinate patch, it could be formulated on a Riemann surface  $C$  with a complex projective structure. In that context,  $\psi(z)$  is interpreted as a section of  $K_C^{-1}$  where  $K_C$  is the canonical bundle,  $P_2(z)$  is a meromorphic quadratic differential while  $P_3(z)$  is a meromorphic cubic differential. In particular, equation (2.1) could be viewed as the quantization of the following Seiberg-Witten curve:

$$\tilde{C} = \{\lambda : \lambda^3 + P_2\lambda + P_3 = 0\} \subset T^*C, \quad (2.2)$$

where  $\lambda$  denotes the Seiberg-Witten differential.

The exact WKB method for  $\text{SL}(3)$ -opers (or higher  $\text{SL}(N)$ -opers) is not yet on solid footing in mathematics, however it was conjectured in [10] that the traditional exact WKB method for Schrödinger equations could be extended to  $\text{SL}(3)$ -opers, by combining the methods developed in [38] with the scaling limit of [4]. Numerical evidence supporting this conjectural picture in certain examples have appeared in [10, 27, 36]. Our description here also builds upon this conjecture; and we will provide further numerical evidence supporting this conjecture in Sections §3 and §4.

## 2.1 The WKB solutions

The exact WKB method is centered around construction of distinguished local WKB solutions, see e.g. [51–53] for the case of Schrödinger equations.

Written in local coordinate  $z$  on a contractible open set  $U \subset C$ , a WKB solution of (2.1) on  $U$  takes the following form:

$$\psi(z) = \exp\left(\frac{1}{\hbar} \int_{z_0}^z \lambda(z) dz\right), \quad (2.3)$$

where  $z_0 \in U$  is a chosen basepoint. For  $\psi(z)$  to be a solution of (2.1),  $\lambda(z)$  must obey the following third-order analogue of the Riccati equation:

$$\lambda^3(z) + 3\hbar\lambda(z)\partial_z\lambda(z) + \hbar^2\partial_z^2\lambda(z) + P_2(z)\lambda(z) + P_3(z) + \frac{1}{2}\hbar P_2'(z) = 0. \quad (2.4)$$

We first build a formal series solution  $\lambda^{\text{formal}}$  in powers of  $\hbar$ . At order- $\hbar^0$ , the Riccati equation (2.4) becomes

$$(\lambda^{(0)})^3 + P_2\lambda^{(0)} + P_3 = 0, \quad (2.5)$$

where  $\lambda^{(0)}$  is the leading order- $\hbar^0$  term in the formal series. Thus we encounter a 3-fold ambiguity; this could be resolved by choosing a solution to (2.5), or equivalently by choosing a sheet  $i$  of the following 3-fold covering of  $C$ :

$$\tilde{C} = \{\lambda^{(0)} : (\lambda^{(0)})^3 + P_2\lambda^{(0)} + P_3 = 0\}. \quad (2.6)$$

In WKB language this is usually called the *WKB curve*, which could be identified with the Seiberg-Witten curve of a 4d  $\mathcal{N} = 2$  theory; in particular  $\lambda^{(0)}$  corresponds to the Seiberg-Witten differential.

Once we have chosen a sheet  $i$  and the corresponding solution  $\lambda_i^{(0)}$  to (2.5), higher order terms in the formal series are determined by solving (2.4) perturbatively in  $\hbar$ . For example, suppose we take  $P_2 = 0$ , then the first few orders in this formal series take the form

$$\begin{aligned}\lambda_i^{\text{formal}} &= \sum_{n=0}^{\infty} \lambda_i^{(n)} \hbar^n \\ &= \lambda_i^{(0)} - \hbar \frac{P'_3}{3P_3} + \hbar^2 \frac{6P_3P_3'' - 7(P'_3)^2}{27P_3^2\lambda_i^{(0)}} + \dots\end{aligned}\tag{2.7}$$

By construction,  $\lambda_i^{\text{formal}}$  is only a formal series in  $\hbar$ , a meaningful question is: under what conditions could one interpret  $\lambda_i^{\text{formal}}$  as an asymptotic series of certain actual solution  $\lambda_i$  to the Ricatti equation, such that  $\lambda_i \sim \lambda_i^{\text{formal}}$  as  $\hbar \rightarrow 0$ ? The conjectural picture is, away from the so-called  *$\theta$ -Stokes curves*, there exist an actual solution  $\lambda_i^\theta$ , such that  $\lambda_i^\theta$  has the desired expansion  $\lambda_i^\theta \sim \lambda_i^{\text{formal}}$  as  $\hbar \rightarrow 0$  while staying within the following closed half-plane

$$\mathbb{H}_\theta = \{\hbar : \text{Re}(e^{-i\theta}\hbar) \geq 0\}.\tag{2.8}$$

The  $\theta$ -Stokes curves are one-dimensional curves on the Riemann surface  $C$ , carrying labels  $ij$ . Along an oriented  $\theta$ -Stokes curve of type  $ij$ ,  $e^{-i\theta}(\lambda_i^{(0)} - \lambda_j^{(0)})dz$  is real and positive. For simplicity suppose the 3-fold covering  $\tilde{C}$  only has simple branch points, then from each branch point there emanate three  $\theta$ -Stokes curves. An important new feature of  $\theta$ -Stokes curves for higher order  $\text{SL}(N)$ -opers, is that a  $\theta$ -Stokes curve of type  $ik$  could be born from the intersection of  $\theta$ -Stokes curves of types  $ij$  and  $jk$  [38, 54, 55]. The collection of  $\theta$ -Stokes curves defines the *Stokes graph*  $W$  at phase  $\theta$ . Examples of Stokes graphs for the  $SU(3)$  equation could be found in Figure 3, Figure 4 and Figure 5. In Figure 1 we give a representative local picture of a Stokes graph in the neighborhood of two simple branch points.

Within a domain that doesn't contain any  $\theta$ -Stokes curves of type  $ij$ , using (2.3) one could integrate the solution  $\lambda_i^\theta(z)$  to the Ricatti equation, obtaining a local WKB solution  $\psi_i^\theta(z)$  to the  $\text{SL}(3)$ -oper equation (2.1). In particular if the domain doesn't contain any  $\theta$ -Stokes curves of any type, we would obtain three WKB solutions  $\psi_{1,2,3}^\theta(z)$ , which give a basis of solutions to the  $\text{SL}(3)$ -oper equation (2.1). As one crosses a  $\theta$ -Stokes curve of type  $ij$ , the WKB solution  $\psi_i^\theta$  jumps by a constant multiple of  $\psi_j^\theta$ . The

rules for gluing together WKB solutions across  $\theta$ -Stokes curves could be formulated in the context of *abelianization* [38, 42], which we describe below.

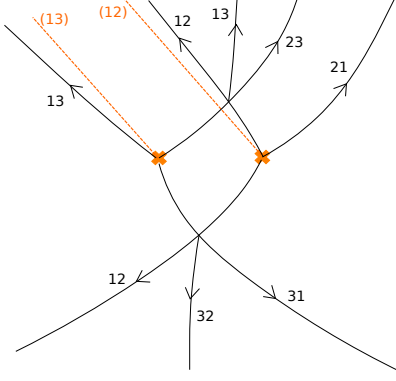


**Figure 1.** A representative local picture of a Stokes graph in the neighborhood of two simple branch points of different types. The orange crosses represent simple branch points, while the orange dashed lines represent the choice of branch cuts.

## 2.2 Abelianization

The  $\text{SL}(3)$ -oper equation (2.1) could be written as a first order differential equation with  $3 \times 3$  matrix coefficients, concretely in a local patch such equation is given as

$$\left[ \partial_z + \hbar^{-1} \begin{pmatrix} 0 & -P_2(z) & P_3(z) + \frac{1}{2}\hbar P_2'(z) \\ 1 & 0 & 0 \\ 0 & 1 & 0 \end{pmatrix} \right] \begin{pmatrix} \hbar^2 \psi''(z) \\ -\hbar \psi'(z) \\ \psi(z) \end{pmatrix} = 0. \quad (2.9)$$

The  $\text{SL}(3)$ -oper equation can therefore be interpreted as a flat  $\text{SL}(3, \mathbb{C})$ -connection  $\nabla$  in a jet bundle over  $C$ .

On the other hand, the WKB ansatz (2.3) could be interpreted as a solution to the following first-order differential equation

$$(\partial_z - \hbar^{-1} \lambda_i^\theta(z)) \psi_i^\theta(z) = 0. \quad (2.10)$$

This is equivalent to say that  $\psi_i^\theta(z)$  corresponds to a flat section of an abelian  $\text{GL}(1, \mathbb{C})$ -connection  $\nabla^{\text{ab}, \theta}$  in a line bundle  $\mathcal{L}$  over the Seiberg-Witten curve  $\tilde{C}$ , where  $i$  labels the sheet index of the covering  $\tilde{C} \rightarrow C$ . As described in [42],  $\nabla^{\text{ab}, \theta}$  has monodromy  $-1$  around branch points of  $\tilde{C} \rightarrow C$ , therefore strictly speaking  $\nabla^{\text{ab}, \theta}$  is an *almost-flat* connection over  $\tilde{C}$ .

From this point of view, finding WKB solutions  $\psi_i^\theta(z)$  to the  $\text{SL}(3)$ -oper equation (2.1), could be reformulated as finding the map from a flat  $\text{SL}(3, \mathbb{C})$ -connections  $\nabla$  over  $C$  to an almost-flat  $\text{GL}(1, \mathbb{C})$ -connection  $\nabla^{\text{ab}, \theta}$  over  $\tilde{C}$ , using the Stokes graph  $W$  at

phase  $\theta$ . Such procedure is denoted as the  $W$ -abelianization of  $\nabla$  and has been studied in [38, 42, 56]. For a given  $\nabla$  and a given Stokes graph  $W$ , there are finitely many  $W$ -abelianizations of  $\nabla$ . For the choice of  $\theta = \arg(\hbar)$ , exact WKB analysis picks up a distinguished  $W$ -abelianization of  $\nabla$  [57].

Concretely, the  $W$ -abelianization procedure spells out a gluing formula for local solutions across  $\theta$ -Stokes curves. Recall that in the complement of the  $\theta$ -Stokes graph, we have bases of local WKB solutions  $\psi_i^\theta$  to the  $\text{SL}(3)$ -oper equation (2.1), however such solutions could be different on the two sides of a  $\theta$ -Stokes curve. One can nevertheless give a gluing map which takes solutions on the left hand side of a  $\theta$ -Stokes curve to solutions on the right hand side. Across a  $\theta$ -Stokes curve of type  $ij$ , the gluing prescription could be summarized as

$$\begin{pmatrix} \psi_i^L \\ \psi_j^L \\ \psi_k^L \end{pmatrix} \mapsto \begin{pmatrix} 1 & x & 0 \\ 0 & 1 & 0 \\ 0 & 0 & 1 \end{pmatrix} \begin{pmatrix} \psi_i^L \\ \psi_j^L \\ \psi_k^L \end{pmatrix} = \begin{pmatrix} \frac{[\psi_i^L, \psi_j^L, \psi_k^L]}{[\psi_i^R, \psi_j^L, \psi_k^L]} \psi_i^R \\ \frac{[\psi_j^L, \psi_k^L, \psi_i^L]}{[\psi_j^R, \psi_k^L, \psi_i^L]} \psi_j^R \\ \frac{[\psi_k^L, \psi_i^L, \psi_j^L]}{[\psi_k^R, \psi_i^L, \psi_j^L]} \psi_k^R \end{pmatrix}, \quad (2.11)$$

where  $x$  is certain constant, and  $[\psi_i, \psi_j, \psi_k]$  denotes the Wronskian of the three solutions.

As we will see in Sections §3 and §4, for special values of  $\theta$  it could happen that a  $\theta$ -Stokes curve of type  $ij$  coincides with a  $\theta$ -Stokes curve of type  $ji$ . In this case, the gluing prescription is chosen to be<sup>7</sup>

$$\begin{pmatrix} \psi_i^L \\ \psi_j^L \\ \psi_k^L \end{pmatrix} \mapsto \begin{pmatrix} z & x & 0 \\ y & z & 0 \\ 0 & 0 & 1 \end{pmatrix} \begin{pmatrix} \psi_i^L \\ \psi_j^L \\ \psi_k^L \end{pmatrix} = \begin{pmatrix} \sqrt{\frac{[\psi_i^L, \psi_j^L, \psi_k^L][\psi_i^L, \psi_j^R, \psi_k^L]}{[\psi_i^R, \psi_j^R, \psi_k^L][\psi_i^R, \psi_j^L, \psi_k^L]}} \psi_i^R \\ \sqrt{\frac{[\psi_j^L, \psi_k^L, \psi_i^L][\psi_j^L, \psi_i^R, \psi_k^L]}{[\psi_j^R, \psi_i^R, \psi_k^L][\psi_j^R, \psi_i^L, \psi_k^L]}} \psi_j^R \\ \frac{[\psi_k^L, \psi_i^L, \psi_j^L]}{[\psi_k^R, \psi_i^L, \psi_j^L]} \psi_k^R \end{pmatrix}, \quad (2.12)$$

where  $z^2 - xy = 1$ .

### 2.3 The spectral coordinates

The spectral coordinates are defined as holonomies of the almost-flat  $\text{GL}(1, \mathbb{C})$ -connection  $\nabla^{\text{ab}, \theta}$  along 1-cycles  $\gamma$  on  $\tilde{C}$ :

$$\mathcal{X}_\gamma^\theta = \text{Hol}_\gamma \nabla^{\text{ab}, \theta} \in \mathbb{C}^\times, \quad \gamma \in H_1(\tilde{C}, \mathbb{Z}). \quad (2.13)$$

---

<sup>7</sup>As described in [10], there are other possible choices for the gluing formula, the one we use here amounts to an “averaged” choice.

By applying the gluing formulas (2.11) and (2.12),  $\mathcal{X}_\gamma^\theta$  can be expressed in terms of Wronskians of local solutions  $\psi_i^\theta(z)$  to the  $\text{SL}(3)$ -oper equation (2.1). For the  $SU(3)$  equation (1.12) considered in this notes, as we will see in Sections §3 and §4, the gluing prescriptions impose relations among local solutions  $\psi_i^\theta(z)$  in different regions separated by  $\theta$ -Stokes curves. After solving such constraints, in the end  $\mathcal{X}_\gamma^\theta$  are expressed in terms of Wronskians of distinguished local solutions: either as asymptotically decaying solutions as  $z$  approaches a singularity, or as eigenvectors of the monodromy around a loop. In this way,  $\mathcal{X}_\gamma^\theta$  are identified with certain coordinate functions on a moduli space of flat  $\text{SL}(3, \mathbb{C})$ -connections. In particular, for certain special loci in the weak-coupling region, as will be described in Section §4, we obtain coordinates of higher length-twist type generalizing complexified Fenchel-Nielsen coordinates [3, 58]. (Higher length-twist coordinates have also been studied in other examples in [8, 27].)

The spectral coordinates depend on the following quantities: the phase  $\theta$ , the Planck's constant  $\hbar$  and the potentials  $P_2$  and  $P_3$  encoding Coulomb branch parameters etc. As long as the topology of  $\theta$ -Stokes graph doesn't change, the dependence on  $\theta$  is trivial. However, in the  $(P_2, P_3, \theta)$  parameter space there is a codimension-1 locus where the topology of  $\theta$ -Stokes graph changes [22, 38]; such locus corresponds to existence of 4d BPS states and is often denoted as the BPS locus. Across the BPS locus,  $\mathcal{X}_\gamma^\theta$  jump by the Kontsevich-Soibelman transformation [22, 38, 45].

The spectral coordinates have nice asymptotic properties: as  $\hbar \rightarrow 0$  in the half plane  $\mathbb{H}_\theta$  defined in (2.8),  $\mathcal{X}_\gamma^\theta$  is expected to admit the following asymptotic expansion [10]:

$$\mathcal{X}_\gamma^\theta \sim \exp \left[ \frac{1}{\hbar} \oint_\gamma \lambda^{\text{formal}} dz \right]. \quad (2.14)$$

If  $\hbar$  is exactly located on the center ray of  $\mathbb{H}_\theta$ , or equivalently  $\theta = \arg(\hbar)$ , then  $\mathcal{X}_\gamma^{\arg(\hbar)}$  have stronger properties [10]. If  $(P_2, P_3, \theta)$  is not on the BPS locus,  $\mathcal{X}_\gamma^{\arg(\hbar)}$  is conjectured to be the Borel summation of the asymptotic expansion (2.14). If  $(P_2, P_3, \theta)$  happens to be on the BPS locus, then the corresponding Borel transform might have singularities<sup>8</sup> and the asymptotic series might not be Borel summable, in which case  $\mathcal{X}_\gamma^{\arg(\hbar)}$  is conjectured to produce the median Borel summation from (2.14). In summary, asymptotic properties of the spectral coordinates enables one to compute Borel resummed quantum periods series (1.8) using abelianization methods.

---

<sup>8</sup>This happens if  $\gamma$  has non-trivial DSZ pairing with the IR charge of the 4d BPS state appearing at the BPS locus.

### 3 The $SU(3)$ equation in the strong-coupling region

From now on, we specialize to the  $SU(3)$  equation (1.12), which corresponds to the quantum Seiberg-Witten curve for 4d  $N = 2$  pure  $SU(3)$  SYM. In this section we focus on the analysis in the strong-coupling region, while in Section §4 we study (1.12) in the weak-coupling region.

#### 3.1 The BPS spectrum

In the strong-coupling region,  $u_1$  and  $u_2$  are small and the BPS spectrum is finite; it consists of 12 BPS states [38, 59]. We choose a positive basis  $\{\gamma_1, \gamma_2, \gamma_3, \gamma_4\}$  for the IR electromagnetic charge lattice. Geometrically  $\gamma_i$  corresponds to homology classes in  $H_1(\tilde{C}, \mathbb{Z})$  where  $\tilde{C}$  is the Seiberg-Witten curve; we show representative cycles in these homology classes in Figure 4. Identifying the Dirac-Schwinger-Zwanziger pairing with the intersection pairing in  $H_1(\tilde{C}, \mathbb{Z})$ , we obtain the following pairing matrix with respect to the chosen basis  $\{\gamma_1, \gamma_2, \gamma_3, \gamma_4\}$ :

$$\begin{pmatrix} 0 & 0 & 1 & -2 \\ 0 & 0 & -2 & 1 \\ -1 & 2 & 0 & 0 \\ 2 & -1 & 0 & 0 \end{pmatrix}. \quad (3.1)$$

The 12 BPS states have the following IR charges:

$$\pm \gamma_1, \pm \gamma_2, \pm \gamma_3, \pm \gamma_4, \pm(\gamma_1 + \gamma_3), \pm(\gamma_2 + \gamma_4). \quad (3.2)$$

If we take  $u_1 = u_2 = 0$ , the BPS spectrum respects a  $\mathbb{Z}_6$  symmetry where BPS states have phases  $0, \pi/3, 2\pi/3, \pi, 4\pi/3, 5\pi/3$  and their central charges have the same norm. This is illustrated in Figure 2.

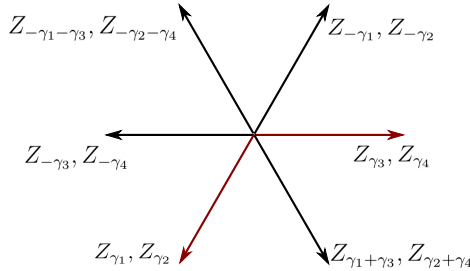


**Figure 2.** Central charges of the 12 BPS states at  $u_1 = u_2 = 0$ .



### 3.2 Stokes graphs

As described in Section §2, the Stokes graph appearing in the exact WKB method depends on a phase parameter  $\theta$ . In particular if  $\theta$  happens to be a phase equal to the central charge phase of a 4d BPS hypermultiplet, the corresponding Stokes graph contains finite segments or webs; while if  $\theta$  happens to be equal to the phase of a 4d BPS vector multiplet, the Stokes graph would contain annulus domain. Such phases are usually called *critical phases*. For example, taking  $u_1 = 0.3, u_2 = 0$  and  $\Lambda = 1$ , in Figure 3 we show the Stokes graphs zoomed in around  $z = 0$ , at critical phases  $\theta \approx 0.3037\pi, 0.6963\pi, \pi$ .<sup>9</sup> (Details of the Stokes graphs at large  $|z|$  are similar to what is shown in Figure 4.)

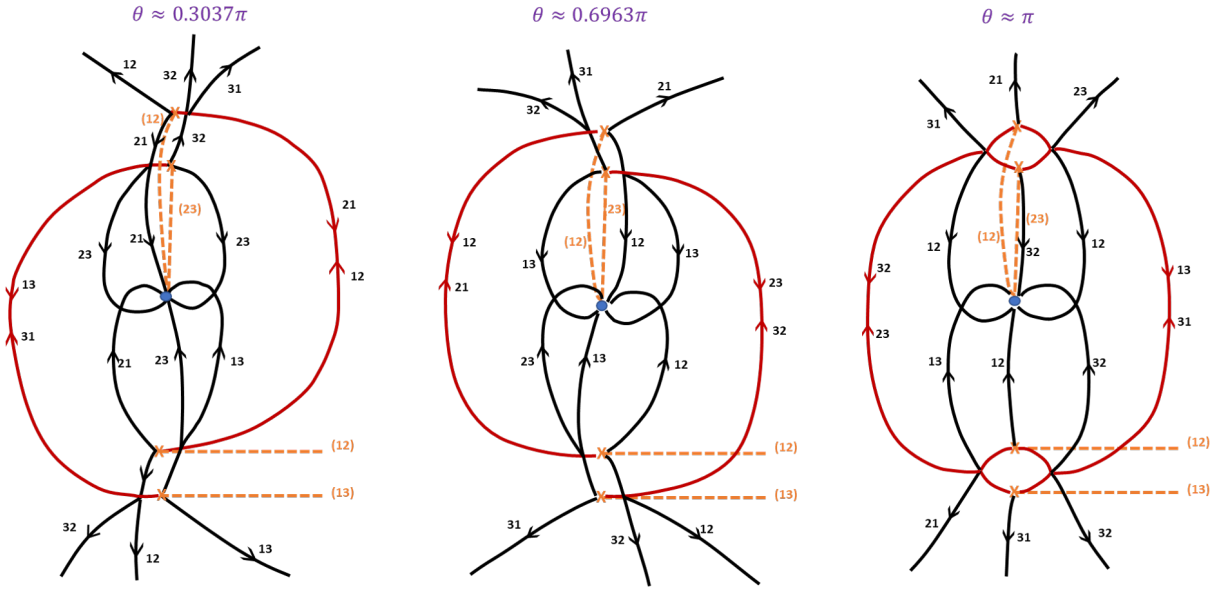


**Figure 3.** Zoomed-in Stokes graphs at  $\theta \approx 0.3037\pi, 0.6963\pi, \pi$ , where we have taken  $u_1 = 0.3, u_2 = 0, \Lambda = 1$  and we focus on details near  $z = 0$ . The irregular singularity at  $z = 0$  is denoted by a blue dot, the irregular singularity at  $z = \infty$  is not shown in the figure. Branch points are represented as orange crosses, while orange dashed lines denote the choice of branch cuts. Finite segments or webs are colored in red; in class  $S$  setup [21, 22, 38] they correspond to trajectories of 6d BPS strings which give rise to 4d BPS states after the twisted compactification on  $C$ .

At  $u_1 = u_2 = 0$  where the BPS spectrum has a  $\mathbb{Z}_6$  symmetry, Stokes graphs at critical phases all look the same, except that the sheet labeling gets permuted. As an example, Figure 4 shows the Stokes graph at  $\theta = \pi/3$ . In the following, we will derive

<sup>9</sup>The Stokes graph at phase  $\theta + \pi$  looks almost identical to that at phase  $\theta$ , except the arrow directions are reversed. Therefore it suffices to consider Stokes graphs at phases within  $(0, \pi]$ .

an expression for the spectral coordinates in terms of distinguished local solutions to the  $SU(3)$  equation (1.12).

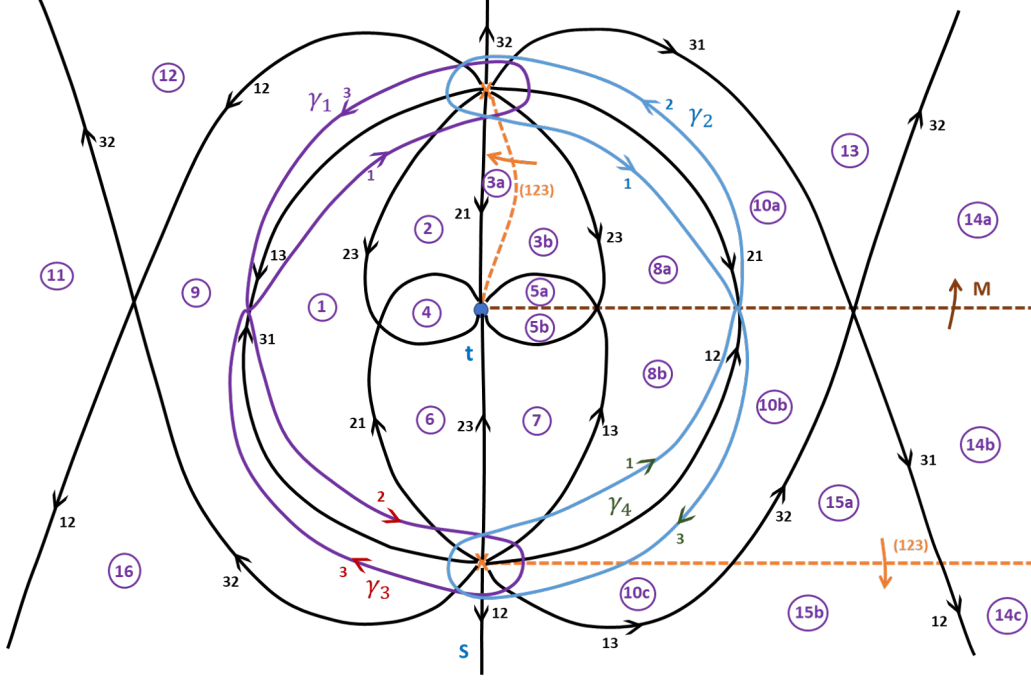


**Figure 4.** The Stokes graph at  $\theta = \pi/3$  with  $u_1 = u_2 = 0$  and  $\Lambda = 1$ . The irregular singularity at  $z = 0$  is represented by a blue dot, while the irregular singularity at  $z = \infty$  is not shown in the figure. Branch points and branch cuts are denoted by orange crosses and orange dashed lines respectively. The monodromy cut is represented by a brown dotted line. We also show representative cycles corresponding to the basis charges  $\gamma_1$ ,  $\gamma_2$ ,  $\gamma_3$  and  $\gamma_4$  in purple, blue, red and green respectively. The Stokes graph divides the punctured-plane into 16 regions, which are labeled by circled purple numbers.

### 3.3 Solving the abelianization problem

The Stokes graph in Figure 4 divides the punctured-plane into 16 regions; in each region we could choose a basis of local WKB solutions to the  $SU(3)$  equation (1.12). In particular there are two distinguished local solutions:

- The local WKB solution  $t$  near  $z = 0$ , characterized as a solution which decays exponentially as  $z \rightarrow 0$  along the negative imaginary axis.
- The local WKB solution  $s$  near  $z = \infty$ , characterized as a solution which decays exponentially as  $z \rightarrow \infty$  along the negative imaginary axis.

Based on the gluing rules in Section §2.2, we could immediately identify a few local WKB solutions in some regions in Figure 4 as  $s$ ,  $t$  or their images under the monodromy actions  $M$  and  $M^{-1}$  around the irregular singularity. However, across the 16 regions there are 10 local WKB solutions which are not straightforwardly related to the distinguished ones; we denote these solutions as  $\psi_i$  ( $i = 1, \dots, 10$ ). The local WKB solutions in the 16 regions are listed in Table 1. Here to write the basis concretely as an ordered tuple we have used the trivialization of  $\tilde{C}$  away from the branch cuts.

region	basis	region	basis
1	$(Mt, s, t)$	2	$(Mt, \psi_1, t)$
3a	$(Mt, \psi_2, t)$	3b	$(\psi_2, t, Mt)$
4	$(Mt, \psi_3, t)$	5a	$(M^2t, t, Mt)$
5b	$(Mt, M^{-1}t, t)$	6	$(Mt, \psi_4, t)$
7	$(Mt, \psi_5, t)$	8a	$(\psi_2, M\psi_5, Mt)$
8b	$(M^{-1}\psi_2, \psi_5, t)$	9	$(\psi_6, s, \psi_7)$
10a	$(Ms, s, Mt)$	10b	$(s, M^{-1}s, t)$
10c	$(t, s, M^{-1}s)$	11	$(Ms, s, M^{-1}s)$
12	$(Ms, s, \psi_7)$	13	$(Ms, s, \psi_8)$
14a	$(Ms, s, \psi_9)$	14b	$(s, M^{-1}s, M^{-1}\psi_9)$
14c	$(M^{-1}\psi_9, s, M^{-1}s)$	15a	$(s, M^{-1}s, \psi_{10})$
15b	$(\psi_{10}, s, M^{-1}s)$	16	$(\psi_6, s, M^{-1}s)$

**Table 1.** Bases of local WKB solutions for the 16 regions shown in Figure 4.

The concrete task of abelianization here, is solving  $\psi_i$  in terms of distinguished local solutions and the monodromy  $M$ . For this purpose, we consider constraints coming from gluing factors across  $\theta$ -Stokes curves. As an example, the gluing factor across the  $\theta$ -Stokes curve of type 13 between regions 3b and 5a indicates that  $\psi_2, Mt, M^2t$  are co-planar in the solution space. Let us denote  $\langle \alpha, \beta \rangle$  as the two-dimensional plane spanned by  $\alpha$  and  $\beta$  in the three-dimensional space of local solutions, then we have  $\langle \psi_2, Mt \rangle = \langle M^2t, Mt \rangle$ . Similarly, the gluing factor across the coincident  $\theta$ -Stokes curves of type 12 and 21 between regions 8a and 10a implies  $\langle \psi_2, M\psi_5 \rangle = \langle Ms, s \rangle$ . For generic  $M$ ,  $\psi_2$  then corresponds to the intersection between  $\langle Ms, s \rangle$  and  $\langle M^2t, Mt \rangle$ . All the

10 local WKB solutions  $\psi_i$  could be determined in a similar fashion:

$$\begin{aligned}
\psi_1 &= \langle s, t \rangle \cap \langle M^2 t, Mt \rangle, & \psi_2 &= \langle Ms, s \rangle \cap \langle M^2 t, Mt \rangle, \\
\psi_3 &= \langle M^2 t, Mt \rangle \cap \langle M^{-1} t, t \rangle, & \psi_4 &= \langle Mt, s \rangle \cap \langle M^{-1} t, t \rangle, \\
\psi_5 &= \langle s, M^{-1} s \rangle \cap \langle M^{-1} t, t \rangle, & \psi_6 &= \langle Ms, s \rangle \cap \langle Mt, t \rangle, \\
\psi_7 &= \langle M^{-1} s, s \rangle \cap \langle Mt, t \rangle, & \psi_8 &= \langle M^{-1} s, s \rangle \cap \langle Mt, Ms \rangle, \\
\psi_9 &= \langle M^{-1} s, s \rangle \cap \langle M^2 s, Ms \rangle, & \psi_{10} &= \langle t, M^{-1} s \rangle \cap \langle Ms, s \rangle.
\end{aligned} \tag{3.3}$$

### 3.4 The spectral coordinates

Let  $\mathcal{X}_{\gamma_i}^{10}$  denote the holonomy of  $\nabla^{\text{ab}, \theta}$  along cycles  $\gamma_i$  shown in Figure 4;  $\mathcal{X}_{\gamma_i}$  are then certain spectral coordinates for the flat  $\text{SL}(3, \mathbb{C})$ -connection  $\nabla$ . We remark that, although the Stokes graph in Figure 4 was drawn at the special point  $u_1 = u_2 = 0$ , the expressions for  $\mathcal{X}_{\gamma_i}$  in terms of distinguished local solutions are expected to hold as we move to small non-zero  $u_{1,2}$ ; the Stokes graph doesn't go through topological changes corresponding to 4d BPS states.

Applying the gluing formulas (2.11) and (2.12), these spectral coordinates are given in terms of Wronskians of distinguished local solutions:

$$\begin{aligned}
\mathcal{X}_{\gamma_1} &= \frac{[Mt, Ms, s][\psi_7, \psi_6, s][t, M^{-1}s, s]}{[\psi_7, s, Ms][t, Mt, s][\psi_6, s, M^{-1}s]}, \\
\mathcal{X}_{\gamma_2} &= \frac{[s, t, Mt][M^{-1}\psi_2, \psi_5, t][s, Mt, t]}{[M^{-1}\psi_2, t, M^{-1}t][Ms, s, Mt][\psi_5, t, Mt]}, \\
\mathcal{X}_{\gamma_3} &= \frac{[\psi_5, s, t][M^{-1}s, s, \psi_6][M^{-1}t, t, M^{-1}\psi_2]}{[\psi_5, t, Mt][M^{-1}s, s, t][M^{-1}s, M^{-1}\psi_2, t]} \sqrt{\frac{[s, Mt, t][\psi_7, Mt, s]}{[\psi_7, s, \psi_6][t, \psi_6, s]}}, \\
\mathcal{X}_{\gamma_4} &= \frac{[\psi_6, t, s][Mt, t, \psi_5][Ms, s, \psi_7]}{[\psi_6, s, M^{-1}s][Mt, t, s][Mt, \psi_7, s]} \sqrt{\frac{[t, M^{-1}s, s][M^{-1}\psi_2, M^{-1}s, t]}{[M^{-1}\psi_2, t, \psi_5][s, \psi_5, t]}},
\end{aligned} \tag{3.4}$$

where  $\psi_{2,5,6,7}$  are intersections of certain planes spanned by the distinguished local solutions  $s, t$  and their images under the monodromy action; they are given explicitly in (3.3).

### 3.5 The asymptotic behavior

As  $\hbar \rightarrow 0$  while staying within the half-plane  $\mathbb{H}_\theta$  defined in (2.8),  $\hbar \log \mathcal{X}_\gamma$  is conjectured to have an asymptotic series expansion given by the formal quantum periods series (1.8). We could perform numerical checks against this conjecture. On the one hand, we

---

<sup>10</sup>From now on, we suppress the dependence on  $\theta$  in the notation for spectral coordinates for compactness reasons.

evaluate (3.4) by numerically solving (1.12) and computing Wronskians of distinguished solutions. On the other hand, we can compute the first few orders in  $\hbar$  of the formal quantum periods  $\Pi_\gamma(\hbar)$ . For example, taking  $u_1 = u_2 = 0$  and  $\Lambda = 1$ , numerical results for  $\hbar = e^{i\pi/3}$  and  $\hbar = \frac{1}{2}e^{i\pi/3}$  are listed in Table 2.

	$\hbar = e^{i\pi/3}$		$\hbar = \frac{1}{2}e^{i\pi/3}$	
	evaluation of (3.4)	$\frac{1}{\hbar}\Pi_\gamma(\hbar)$ at $o(\hbar^6)$	evaluation of (3.4)	$\frac{1}{\hbar}\Pi_\gamma(\hbar)$ at $o(\hbar^6)$
$\log \mathcal{X}_{\gamma_1}$	-3.5756	-3.5873	-10.2481	-10.2482
$\log \mathcal{X}_{\gamma_2}$	-3.5756	-3.5873	-10.2481	-10.2482
$\log \mathcal{X}_{\gamma_3}$	1.7878 - 0.4490i	1.7937 - 0.4405i	5.12405 + 1.88253i	5.12412 + 1.88266i
$\log \mathcal{X}_{\gamma_4}$	1.7878 - 0.4490i	1.7937 - 0.4405i	5.12405 + 1.88253i	5.12412 + 1.88266i

**Table 2.** Comparison of  $\log \mathcal{X}_\gamma$  with the formal quantum periods expansion up to order- $\hbar^6$  at  $\hbar = e^{i\pi/3}$  and  $\hbar = \frac{1}{2}e^{i\pi/3}$ , where we have set  $u_1 = u_2 = 0$  and  $\Lambda = 1$ .

From Table 2 we see that as  $|\hbar|$  gets smaller, the spectral coordinates obtained via abelianization method get closer to the truncated quantum periods expansion<sup>11</sup>. This is in line with the conjectured asymptotic behavior of spectral coordinates. Unfortunately numerical evaluation of (3.4) becomes rather difficult for small  $|\hbar|$ ; we are not able to demonstrate the asymptotic behavior at smaller  $|\hbar|$ . Nevertheless we regard Table 2 as evidence that higher-order exact WKB methods indeed works. As a further remark, we notice that the system has a symmetry where  $\mathcal{X}_{\gamma_1} = \mathcal{X}_{\gamma_2}$  and  $\mathcal{X}_{\gamma_3} = \mathcal{X}_{\gamma_4}$ . The numerical values in Table 2 do respect such symmetry, which could serve as an extra consistency check for our analysis.

Finally we mention that, for  $\arg(\hbar) = \pi/3$  which is the phase  $\theta$  for the Stokes graph in Figure 4,  $\hbar \log \mathcal{X}_{\gamma_{1,2}}$  are conjectured to be the Borel resummation of  $\Pi_{\gamma_{1,2}}(\hbar)$ ; while  $\hbar \log \mathcal{X}_{\gamma_{3,4}}$  are conjectured to be the median Borel resummation of  $\Pi_{\gamma_{3,4}}(\hbar)$ , as the latter are not Borel summable. We expect to explore the structures of Borel transforms and resummations for quantum periods in more detail in [16].

---

<sup>11</sup>One would expect the agreement to get better by including a few more higher order terms in  $\hbar$ . An efficient way of computing quantum periods series to high orders in  $\hbar$  is the so-called *quantum operator* approach [11, 41]. It would be very interesting to generalize such method to higher rank theories.

## 4 The $SU(3)$ equation in the weak-coupling region

### 4.1 A Stokes graph

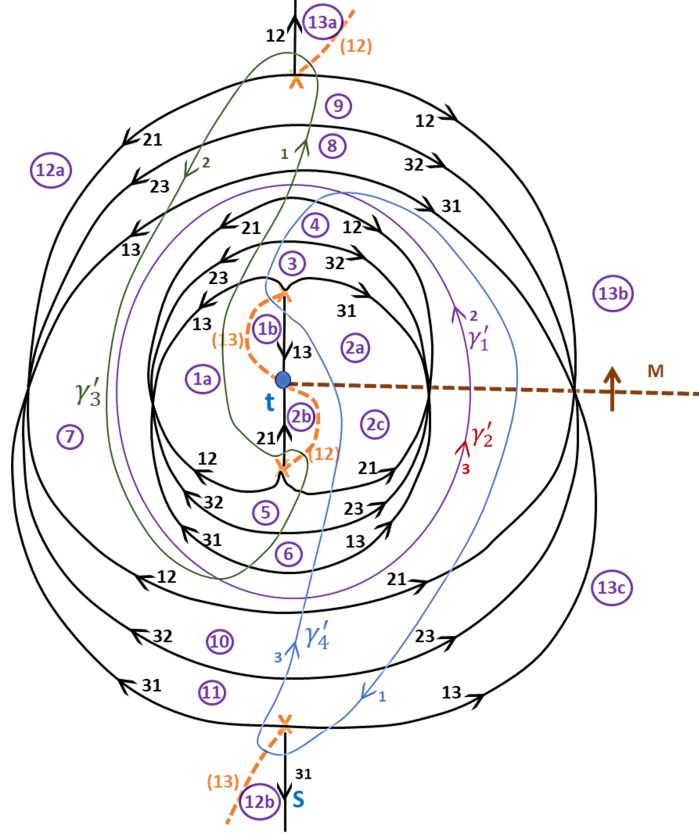


**Figure 5.** The Stokes graph at  $\theta = 0$ , with  $u_1 = 4.5$ ,  $u_2 = 0$  and  $\Lambda = 1$ . The notation conventions are the same as those in Figure 4. We show representative cycles corresponding to the basis charges  $\gamma'_1$ ,  $\gamma'_2$ ,  $\gamma'_3$  and  $\gamma'_4$  in purple, red, green and blue respectively. This Stokes graph divides the punctured-plane into 13 regions.

Now we turn our attention to the weak-coupling region, where the BPS spectrum becomes very complicated [59]. In particular we consider parameters under which a Stokes graph of the higher length-twist type [27] appears. Our motivation for considering such Stokes graphs is, as briefly described in Section §1.2.3, to make connections with gauge theory calculations. The corresponding spectral coordinates are higher length-twist coordinates, which are closely related to the quantum  $a$  and  $a_D$  periods. In this paper we construct the higher length-twist coordinates using abelianization methods, while perspectives from instanton calculus will be investigated in [16].

Taking  $\Lambda = 1$ ,  $u_2 = 0$ , and real  $u_1 > 1.25$ , at  $\theta = 0$  the Stokes graph looks like Figure 5. In particular we see a ring domain corresponding to the  $W$ -bosons; this ring

domain is denoted as the region 7 in Figure 5. We choose a basis  $\{\gamma'_1, \gamma'_2, \gamma'_3, \gamma'_4\}$  of the IR charge lattice, as shown in Figure 5. This basis is more natural for the analysis in the weak-coupling region. We will write down the corresponding spectral coordinates  $\mathcal{X}_{\gamma'_i}$  in Section §4.3; in particular  $\mathcal{X}_{\gamma'_{1,2}}$  are higher length coordinates and  $\mathcal{X}_{\gamma'_{3,4}}$  are higher twist coordinates.

## 4.2 Solving the abelianization problem

The Stokes graph in Figure 5 divides the punctured-plane into 13 regions. The local WKB solutions in each region turn out to be expressed in terms of the following distinguished local solutions:

- The local WKB solution  $t$  near  $z = 0$  and the local WKB solution  $s$  near  $z = \infty$ , characterized as exponentially decaying solution as  $z \rightarrow 0$  and  $z \rightarrow \infty$  respectively, along the negative imaginary axis.
- Eigenvectors  $\alpha$ ,  $\beta$  and  $\gamma$  of the counterclockwise monodromy  $M$  around  $z = 0$ . For the parameter range we consider here, namely real  $u_1 > 1.25$ ,  $u_2 = 0$  and  $\hbar \in \mathbb{R}_+$ , the eigenvalues of the monodromy  $M$  are all real and positive, moreover one of the eigenvalues is 1. Let us denote the eigenvalues of  $M$  as  $\mu_\alpha$ ,  $\mu_\beta$  and  $\mu_\gamma$ , corresponding to the eigenvectors  $\alpha$ ,  $\beta$  and  $\gamma$  respectively. Then  $\alpha$ ,  $\beta$  and  $\gamma$  are specified according to the condition  $\mu_\alpha = 1$ ,  $\mu_\beta > 1$  and  $\mu_\gamma < 1$ .<sup>12</sup>

We proceed by first listing bases of local WKB solutions for each region in Table 3; in this case there are 14 local solutions  $\phi_i$  not straightforwardly related to the above distinguished solutions and their images under the monodromy action.

Similar to the strong coupling case described in Section §3.3, by exploring the constraints imposed by the gluing condition we could solve for  $\phi_i$ . The solutions are given as follows:

$$\begin{aligned}
\phi_1 &= \langle t, Mt \rangle \cap \langle M^{-2}t, M^{-1}t \rangle, & \phi_2 &= \langle t, M^{-1}t \rangle \cap \langle \alpha, \beta \rangle, \\
\phi_3 &= \langle t, M^{-1}t \rangle \cap \langle Mt, \gamma \rangle, & \phi_4 &= \langle Mt, \gamma \rangle \cap \langle \alpha, \beta \rangle, \\
\phi_5 &= \langle t, Mt \rangle \cap \langle \alpha, \gamma \rangle, & \phi_6 &= \langle t, Mt \rangle \cap \langle M^{-1}t, \beta \rangle, \\
\phi_7 &= \langle M^{-1}t, \beta \rangle \cap \langle \alpha, \gamma \rangle, & \phi_8 &= \langle \alpha, \gamma \rangle \cap \langle Ms, M^2s \rangle, \\
\phi_9 &= \langle \alpha, \gamma \rangle \cap \langle \beta, s \rangle, & \phi_{10} &= \langle \beta, s \rangle \cap \langle Ms, M^2s \rangle, \\
\phi_{11} &= \langle \alpha, \beta \rangle \cap \langle s, M^{-1}s \rangle, & \phi_{12} &= \langle \alpha, \beta \rangle \cap \langle Ms, \gamma \rangle, \\
\phi_{13} &= \langle Ms, \gamma \rangle \cap \langle s, M^{-1}s \rangle, & \phi_{14} &= \langle s, M^{-1}s \rangle \cap \langle M^2s, Ms \rangle.
\end{aligned} \tag{4.1}$$

---

<sup>12</sup>One might wonder where this particular specification for  $\alpha$ ,  $\beta$  and  $\gamma$  comes from; after all, given a generic monodromy matrix  $M$  we have 6 ways of defining  $(\alpha, \beta, \gamma)$ . The choice we take here is the one which matches the leading asymptotic behavior of spectral coordinates, given by the classical periods around the ring domain.

region	basis	region	basis
1a	$(t, Mt, M^{-1}t)$	1b	$(M^{-1}t, Mt, t)$
2a	$(M\phi_1, Mt, t)$	2b	$(t, \phi_1, M^{-1}t)$
2c	$(\phi_1, t, M^{-1}t)$	3	$(\phi_2, Mt, \phi_3)$
4	$(\phi_2, \phi_4, \gamma)$	5	$(\phi_5, \phi_6, M^{-1}t)$
6	$(\phi_5, \beta, \phi_7)$	7	$(\alpha, \beta, \gamma)$
8	$(\phi_8, \beta, \phi_9)$	9	$(\phi_8, \phi_{10}, s)$
10	$(\phi_{11}, \phi_{12}, \gamma)$	11	$(\phi_{11}, Ms, \phi_{13})$
12a	$(\phi_{14}, Ms, s)$	12b	$(s, Ms, \phi_{14})$
13a	$(M^2s, Ms, s)$	13b	$(Ms, M^2s, s)$
13c	$(s, Ms, M^{-1}s)$		

**Table 3.** Bases of local WKB solutions for the 13 regions shown in [Figure 5](#).

### 4.3 The spectral coordinates

The spectral coordinates  $\mathcal{X}_{\gamma'_{1,2}}$  could be identified with the higher length coordinates on the moduli space of flat  $\mathrm{SL}(3, \mathbb{C})$ -connections; they are simply given by the corresponding eigenvalues of the monodromy action:

$$\mathcal{X}_{\gamma'_1} = \mu_\beta, \quad \mathcal{X}_{\gamma'_2} = \mu_\gamma \quad (4.2)$$

The spectral coordinates  $\mathcal{X}_{\gamma'_{3,4}}$  are higher twist coordinates; we express them via Wronskians of distinguished local solutions:

$$\begin{aligned}
\mathcal{X}_{\gamma'_3} &= \sqrt{-\frac{[Ms, \phi_{14}, s][Ms, \phi_8, s][\phi_{10}, \phi_9, \phi_8][\beta, \phi_7, \phi_5][\beta, M^{-1}t, \phi_5][\phi_6, \phi_1, M^{-1}t][t, M^{-1}t, Mt]}{[\phi_{10}, \phi_{14}, s][\beta, \phi_9, \phi_8][\beta, s, \phi_8][\phi_6, \phi_7, \phi_5][t, \phi_1, M^{-1}t][t, \phi_5, M^{-1}t][\phi_2, \phi_3, Mt]}} \\
&\quad \times \sqrt{\frac{[t, \phi_3, Mt][\phi_2, \phi_4, \gamma][\phi_2, \beta, \gamma][\alpha, \phi_9, \beta][\phi_8, \phi_{10}, s][\phi_8, M^2s, s]}{[\phi_2, M^{-1}t, Mt][\alpha, \phi_4, \gamma][\phi_8, \phi_9, \beta][\phi_8, \gamma, \beta][Ms, M^2s, s][Ms, \phi_{10}, s]}}, \\
\mathcal{X}_{\gamma'_4} &= \frac{1}{\mu_\alpha} \sqrt{\frac{[s, \phi_{14}, Ms][s, \phi_{11}, Ms][\phi_{13}, \phi_{12}, \phi_{11}][\gamma, \alpha, \beta][\gamma, \phi_5, \beta][\phi_7, \phi_6, \phi_5][t, M^{-1}t, Mt]}{[\phi_{13}, \phi_{14}, Ms][\gamma, \phi_{12}, \phi_{11}][\gamma, Ms, \phi_{11}][\phi_7, \alpha, \beta][M^{-1}t, \phi_6, \phi_5][M^{-1}t, \beta, \phi_5][\phi_2, \phi_3, Mt]}} \\
&\quad \times \sqrt{\frac{[t, \phi_3, Mt][\phi_2, \phi_4, \gamma][\phi_2, \beta, \gamma][\alpha, \phi_{12}, \gamma][\phi_{11}, \phi_{13}, Ms][\phi_{11}, M^{-1}s, Ms]}{[\phi_2, M^{-1}t, Mt][\alpha, \phi_4, \gamma][\phi_{11}, \phi_{12}, \gamma][\phi_{11}, \beta, \gamma][s, M^{-1}s, Ms][s, \phi_{13}, Ms]}}, \quad (4.3)
\end{aligned}$$

where the local WKB solutions  $\phi_i$  are given in [\(4.1\)](#).

The expressions in [\(4.3\)](#) look rather formidable. As a consistency check and an application, we consider the exact quantization condition (EQC) for a spectral problem



relevant to the  $SU(3)$  equation (1.12). Imagine we would like to study certain bound state solution to (1.12) living along a one-dimensional path between  $z = 0$  and  $z = \infty$ , where the solution decays as  $z$  approaches 0 and  $\infty$ . For example, suppose the one-dimensional path goes into  $z = 0$  and  $z = \infty$  along the negative imaginary axis, then the condition for existence of such bound states is that the distinguished solution  $s$  decaying into  $z = 0$  is proportional to the distinguished solution  $t$  decaying into  $z = \infty$ . Substituting this condition into (4.3), the complicated-looking expressions simply to

$$\frac{1}{\mu_\beta} \mathcal{X}_{\gamma'_3} = 1, \quad \mu_\beta \mathcal{X}_{\gamma'_4} = 1. \quad (4.4)$$

Equation (4.4) is regarded as the EQC for such bound states.

In [30] the authors studied EQC for a family of exactly solvable deformed Hamiltonians, obtained by quantizing the Seiberg-Witten curve for 4d  $N = 2$   $SU(N)$  SYM in the hyperelliptic form. In the case of  $SU(3)$  SYM, the Seiberg-Witten curve we use here comes from class  $S$  construction; it is in the dual parametrization of the Seiberg-Witten curve considered in [30]. It would be interesting to straighten out the relation between (4.4) and the EQC in [30] derived from certain 4d limit of TS/ST correspondence.

#### 4.4 The asymptotic behavior

Similar to Section §3.5, here we perform numerical checks against the asymptotic behavior of spectral coordinates. For example, taking  $u_1 = 4.5$ ,  $u_2 = 0$  and  $\Lambda = 1$ , numerical results for  $\hbar = 1$  and  $\hbar = 0.8$  are listed in Table 4.

	$\hbar = 1$		$\hbar = 0.8$	
	evaluation	$\frac{1}{\hbar} \Pi_{\gamma'}(\hbar)$ at $o(\hbar^2)$	evaluation	$\frac{1}{\hbar} \Pi_{\gamma'}(\hbar)$ at $o(\hbar^2)$
$\log \mathcal{X}_{\gamma'_1}$	11.90	11.98	15.59	15.63
$\log \mathcal{X}_{\gamma'_2}$	-11.90	-11.98	-15.59	-15.63
$\log \mathcal{X}_{\gamma'_3}$	$5.93 + 0.94i$	$5.99 + 0.96i$	$7.78 + 2.01i$	$7.81 + 2.02i$
$\log \mathcal{X}_{\gamma'_4}$	$-5.93 - 0.94i$	$-5.99 - 0.96i$	$-7.78 - 2.01i$	$-7.81 - 2.02i$

**Table 4.** Comparison of  $\log \mathcal{X}_{\gamma'}$  with the formal quantum periods expansion up to order- $\hbar^2$  at  $\hbar = 1$  and  $\hbar = 0.8$ , where we have set  $u_1 = 4.5$ ,  $u_2 = 0$  and  $\Lambda = 1$ .

In the evaluation of  $\log \mathcal{X}_{\gamma'}$  using (4.2) and (4.3), similar to what happens in the strong coupling region, we found it difficult to perform numerical evaluation at small  $\hbar$ . Compared to the strong coupling region, here the numerical evaluation contains an extra step, namely diagonalizing the monodromy matrix  $M$  and finding its eigenvalues and eigenvectors. As  $\hbar$  gets rather small, one of the eigenvalues for  $M$  becomes very small, introducing further difficulty in the numerical analysis. Nevertheless, from

Table 4 one can see as  $\hbar$  goes from 1 to 0.8,  $\hbar \log \mathcal{X}_{\gamma'}$  becomes closer to the truncated quantum periods expansion, where the discrepancy decreases from about 1% to about 0.3%. This provides evidence for the conjectured asymptotic behavior of spectral coordinates.

## Acknowledgement

We thank Dylan Allegretti, Alba Grassi, Saebyeok Jeong, Dustin Lorshbough, Gregory Moore and Andrew Neitzke for very helpful discussions. FY is supported by DOE grant DE-SC0010008.

## References

- [1] N. A. Nekrasov and S. L. Shatashvili, “Quantization of Integrable Systems and Four Dimensional Gauge Theories,” in *16th International Congress on Mathematical Physics*, pp. 265–289. 8, 2009. [0908.4052](#).
- [2] L. F. Alday, D. Gaiotto, and Y. Tachikawa, “Liouville Correlation Functions from Four-dimensional Gauge Theories,” *Lett. Math. Phys.* **91** (2010) 167–197, [0906.3219](#).
- [3] N. Nekrasov, A. Rosly, and S. Shatashvili, “Darboux coordinates, Yang-Yang functional, and gauge theory,” *Nucl. Phys. B Proc. Suppl.* **216** (2011) 69–93, [1103.3919](#).
- [4] D. Gaiotto, “Opers and TBA,” [1403.6137](#).
- [5] A. Grassi, Y. Hatsuda, and M. Marino, “Topological Strings from Quantum Mechanics,” *Annales Henri Poincaré* **17** (2016), no. 11, 3177–3235, [1410.3382](#).
- [6] M. Marino, “Spectral Theory and Mirror Symmetry,” *Proc. Symp. Pure Math.* **98** (2018) 259, [1506.07757](#).
- [7] N. Nekrasov, “BPS/CFT correspondence: non-perturbative Dyson-Schwinger equations and qq-characters,” *JHEP* **03** (2016) 181, [1512.05388](#).
- [8] S. Jeong and N. Nekrasov, “Opers, surface defects, and Yang-Yang functional,” [1806.08270](#).
- [9] K. Ito, M. Mariño, and H. Shu, “TBA equations and resurgent Quantum Mechanics,” *JHEP* **01** (2019) 228, [1811.04812](#).
- [10] L. Hollands and A. Neitzke, “Exact WKB and abelianization for the  $T_3$  equation,” [1906.04271](#).
- [11] A. Grassi, J. Gu, and M. Mariño, “Non-perturbative approaches to the quantum Seiberg-Witten curve,” *JHEP* **07** (2020) 106, [1908.07065](#).

- [12] S. Jeong and N. Nekrasov, “Riemann-Hilbert correspondence and blown up surface defects,” *JHEP* **12** (2020) 006, [2007.03660](#).
- [13] N. Lee and N. Nekrasov, “Quantum Spin Systems and Supersymmetric Gauge Theories, I,” [2009.11199](#).
- [14] N. Seiberg and E. Witten, “Electric-magnetic duality, monopole condensation, and confinement in  $n=2$  supersymmetric yang-mills theory,” *Nuclear Physics B* **426** (Sep, 1994) 19–52.
- [15] N. Seiberg and E. Witten, “Monopoles, duality and chiral symmetry breaking in  $n = 2$  supersymmetric qcd,” *Nuclear Physics B* **431** (Dec, 1994) 484–550.
- [16] F. Yan, “Exact WKB and the quantum Seiberg-Witten curve for 4d  $N = 2$  pure  $SU(3)$  Yang-Mills, Part II,” *Work in progress*.
- [17] N. A. Nekrasov and S. L. Shatashvili, “Supersymmetric vacua and Bethe ansatz,” *Nucl. Phys. B Proc. Suppl.* **192-193** (2009) 91–112, [0901.4744](#).
- [18] N. A. Nekrasov and S. L. Shatashvili, “Quantum integrability and supersymmetric vacua,” *Prog. Theor. Phys. Suppl.* **177** (2009) 105–119, [0901.4748](#).
- [19] N. A. Nekrasov, “Seiberg-Witten prepotential from instanton counting,” *Adv. Theor. Math. Phys.* **7** (2003), no. 5, 831–864, [hep-th/0206161](#).
- [20] N. Nekrasov and A. Okounkov, “Seiberg-Witten theory and random partitions,” *Prog. Math.* **244** (2006) 525–596, [hep-th/0306238](#).
- [21] D. Gaiotto, G. W. Moore, and A. Neitzke, “Wall-crossing, Hitchin Systems, and the WKB Approximation,” [0907.3987](#).
- [22] D. Gaiotto, “ $N=2$  dualities,” *JHEP* **08** (2012) 034, [0904.2715](#).
- [23] N. Nekrasov and E. Witten, “The Omega Deformation, Branes, Integrability, and Liouville Theory,” *JHEP* **09** (2010) 092, [1002.0888](#).
- [24] N. Hitchin, “Stable bundles and integrable systems,” *Duke Math. J.* **54** (1987), no. 1, 91–114.
- [25] A. Beilinson and V. Drinfeld, “Opers,” *arXiv Mathematics e-prints* (Jan., 2005) [math/0501398](#), [math/0501398](#).
- [26] W. Fenchel, J. Nielsen, and A. L. Schmidt, *Discontinuous Groups of Isometries in the Hyperbolic Plane*. De Gruyter, Berlin, Boston, 12 May. 2011.
- [27] L. Hollands and O. Kidwai, “Higher length-twist coordinates, generalized Heun’s opers, and twisted superpotentials,” *Adv. Theor. Math. Phys.* **22** (2018) 1713–1822, [1710.04438](#).
- [28] S. Codesido, A. Grassi, and M. Marino, “Spectral Theory and Mirror Curves of Higher Genus,” *Annales Henri Poincaré* **18** (2017), no. 2, 559–622, [1507.02096](#).

- [29] S. H. Katz, A. Klemm, and C. Vafa, “Geometric engineering of quantum field theories,” *Nucl. Phys. B* **497** (1997) 173–195, [hep-th/9609239](#).
- [30] A. Grassi and M. Mariño, “A Solvable Deformation of Quantum Mechanics,” *SIGMA* **15** (2019) 025, [1806.01407](#).
- [31] P. C. Argyres and A. E. Faraggi, “The vacuum structure and spectrum of N=2 supersymmetric SU(n) gauge theory,” *Phys. Rev. Lett.* **74** (1995) 3931–3934, [hep-th/9411057](#).
- [32] A. Klemm, W. Lerche, S. Yankielowicz, and S. Theisen, “Simple singularities and N=2 supersymmetric Yang-Mills theory,” *Phys. Lett. B* **344** (1995) 169–175, [hep-th/9411048](#).
- [33] A. Klemm, W. Lerche, and S. Theisen, “Nonperturbative effective actions of N=2 supersymmetric gauge theories,” *Int. J. Mod. Phys. A* **11** (1996) 1929–1974, [hep-th/9505150](#).
- [34] K. Ito and H. Shu, “ODE/IM correspondence and the Argyres-Douglas theory,” *JHEP* **08** (2017) 071, [1707.03596](#).
- [35] K. Ito and H. Shu, “TBA equations for the Schrodinger equation with a regular singularity,” [1910.09406](#).
- [36] D. Dumas and A. Neitzke, “Opers and nonabelian Hodge: numerical studies,” [2007.00503](#).
- [37] O. Dumitrescu, L. Fredrickson, G. Kydonakis, R. Mazzeo, M. Mulase, and A. Neitzke, “Opers versus nonabelian Hodge,” *arXiv e-prints* (July, 2016) arXiv:1607.02172, [1607.02172](#).
- [38] D. Gaiotto, G. W. Moore, and A. Neitzke, “Spectral networks,” *Annales Henri Poincare* **14** (2013) 1643–1731, [1204.4824](#).
- [39] V. A. Balian R., Parisi G., “Quartic oscillator. in: Albeverio s. et al. (eds) feynman path integrals.,” *Lecture Notes in Physics* **106** (1979).
- [40] S. Codesido and M. Marino, “Holomorphic Anomaly and Quantum Mechanics,” *J. Phys. A* **51** (2018), no. 5, 055402, [1612.07687](#).
- [41] M.-x. Huang, “On Gauge Theory and Topological String in Nekrasov-Shatashvili Limit,” *JHEP* **06** (2012) 152, [1205.3652](#).
- [42] L. Hollands and A. Neitzke, “Spectral Networks and Fenchel–Nielsen Coordinates,” *Lett. Math. Phys.* **106** (2016), no. 6, 811–877, [1312.2979](#).
- [43] V. V. Fock and A. B. Goncharov, “Moduli spaces of local systems and higher Teichmuller theory,” *arXiv Mathematics e-prints* (Nov., 2003) math/0311149, [math/0311149](#).

- [44] D. Gaiotto, G. W. Moore, and A. Neitzke, “Four-dimensional wall-crossing via three-dimensional field theory,” *Commun. Math. Phys.* **299** (2010) 163–224, [0807.4723](#).
- [45] M. Kontsevich and Y. Soibelman, “Stability structures, motivic Donaldson-Thomas invariants and cluster transformations,” [0811.2435](#).
- [46] A. Mironov and A. Morozov, “Nekrasov Functions and Exact Bohr-Zommerfeld Integrals,” *JHEP* **04** (2010) 040, [0910.5670](#).
- [47] R. Flume, F. Fucito, J. F. Morales, and R. Poghossian, “Matone’s relation in the presence of gravitational couplings,” *JHEP* **04** (2004) 008, [hep-th/0403057](#).
- [48] M. Aganagic, M. C. Cheng, R. Dijkgraaf, D. Krefl, and C. Vafa, “Quantum Geometry of Refined Topological Strings,” *JHEP* **11** (2012) 019, [1105.0630](#).
- [49] A. S. Losev, A. Marshakov, and N. A. Nekrasov, “Small instantons, little strings and free fermions,” in *From Fields to Strings: Circumnavigating Theoretical Physics: A Conference in Tribute to Ian Kogan*, pp. 581–621. 2, 2003. [hep-th/0302191](#).
- [50] D. Fioravanti, H. Poghosyan, and R. Poghossian, “ $T$ ,  $Q$  and periods in  $SU(3)$   $N = 2$  SYM,” *JHEP* **03** (2020) 049, [1909.11100](#).
- [51] A. Voros, “The return of the quartic oscillator. the complex wkb method,” *Annales de l’I.H.P. Physique théorique* **39** (1983), no. 3, 211–338.
- [52] E. Delabaere, H. Dillinger, and F. Pham, “Exact semiclassical expansions for one-dimensional quantum oscillators,” *Journal of Mathematical Physics* **38** (1997) 6126–6184.
- [53] K. Iwaki and T. Nakanishi, “Exact wkb analysis and cluster algebras,” *arXiv: Classical Analysis and ODEs* (2014).
- [54] T. Aoki, T. Kawai, and Y. Takei, *New Turning Points in the Exact WKB Analysis for Higher-order Ordinary Differential Equations*. Technical report. Kyoto University, Research Institute for Mathematical Sciences, 1991.
- [55] T. Aoki, T. Kawai, S. Sasaki, A. Shudo, and Y. Takei, “Virtual turning points and bifurcation of stokes curves for higher order ordinary differential equations,” *Journal of Physics A: Mathematical and General* **38** (Mar, 2005) 3317–3336.
- [56] N. Nikolaev, “Abelianisation of logarithmic  $\mathfrak{sl}_2$ -connections,” 2019.
- [57] A. Neitzke and N. Nikolaev *Work in progress*.
- [58] Y. Kabaya, “Parametrization of  $\mathrm{psl}(2, \mathbb{C})$ -representations of surface groups,” 2013.
- [59] D. Galakhov, P. Longhi, T. Mainiero, G. W. Moore, and A. Neitzke, “Wild Wall Crossing and BPS Giants,” *JHEP* **11** (2013) 046, [1305.5454](#).